Cell Reports, Volume *30*

Supplemental Information

Targeting the Oncogenic Long Non-coding RNA *SLNCR1* by Blocking Its Sequence-Specific Binding to the Androgen Receptor

Karyn Schmidt, Chase A. Weidmann, Thomas A. Hilimire, Elaine Yee, Breanne M. Hatfield, John S. Schneekloth Jr., Kevin M. Weeks, and Carl D. Novina

Sequence	Name	Type
CT**TC**CCACCCTGGTCTTCTCCTGTAA	*SLNCR1*$^{\text{AR MUT 1}}$ Forward	SDM
GG**GA**AGGGAAAAATACCTCCAGCTTGGC	*SLNCR1*$^{\text{AR MUT 1}}$ Reverse	SDM
T**AG**TCTC**AG**GTAACGTGTGGCCGCCTTTTC	*SLNCR1*$^{\text{AR MUT 2}}$ Forward	SDM
C**CT**GAGA**CT**ACCAGGGTGGAGAGGGAAAAATACC	*SLNCR1*$^{\text{AR MUT 2}}$ Reverse	SDM
C**CT**GAGA**CT**ACCAGGGTGG**GA**AGGGAAAAATACC	*SLNCR1*$^{\text{AR MUT 1 and 2}}$ Forward	SDM
CT**TC**CCACCCTGGT**AG**TCTC**AG**GTAA	*SLNCR1*$^{\text{AR MUT 1 and 2}}$ Reverse	SDM
GAGAACGTGGTGGAATCAGA	*SLNCR* Forward	qPCR
TCCCATCCTCTTTCTTGTCC	*SLNCR* Reverse	qPCR
CGAACTTTGACAGCGACAAG	*MMP9* Forward	qPCR
CACTGAGGAATGATCTAAGCCC	*MMP9* Reverse	qPCR
GAAGGTGAAGGTCGGAGT	*GAPDH* Forward	qPCR
GAAGATGGTGATGGGATTTC	*GAPDH* Reverse	qPCR
CTTTAGAGGCGCTGACATCC	*HOXA11AS-203* Forward	qPCR
AGAAATGGAACTCGGACTTGG	*HOXA11AS-203* Reverse	qPCR
ATCAGCTAGCATGGATTACAAGGATGACGACGATAAGG GCGGAGGGATACCGGTATCG	Duplexed primer to insert ATG, FLAG tag and 3x glycine linker into pEGFP-C1-AR	cloning
CGATACCGGTATCCCTCCGCCCTTATCGTCGTCATCCTT GTAATCCATGCTAGCTGAT	Duplexed primer to insert ATG, FLAG tag and 3x glycine linker into pEGFP-C1-AR	cloning
GGATCAGTCCTTCCCATCC	*SLNCR*^{cons} RT primer	MaP
GACTGGAGTTCAGACGTGTGCTCTTCCGATCTNNNNNA CCTCCGCGAGTCTGG	*SLNCR*^{cons} step 1 Forward	MaP
CCCTACACGACGCTCTTCCGATCTNNNNNGGATCAGTC CTTCCCATCC	*SLNCR*^{cons} step 1 Reverse	MaP
CAAGCAGAAGACGGCATACGAG-(index)8-GTGACTGGAGTTCAGAC	TruSeq LT step 2 index Forward	MaP
AATGATACGGCGACCACCGAGATCTACACTCTTTCCCT ACACGACGCTCTTCCGATCT	TruSeq LT step 2 Reverse	MaP
CAGGGGAAAGCGCGAA	U1 RT primer	MaP
GACTGGAGTTCAGACGTGTGCTCTTCCGATCTNNNNNA TACTTACCTGGCA	U1 step 1 Forward	MaP
CCCTACACGACGCTCTTCCGATCTNNNNNCAGGGGAAA GCGCGAA	U1 step 1 Reverse	MaP

Table S1: Oligos used in this study. Related to STAR Methods. SDM = site-directed mutagenesis primers. Mutations from wild-type *SLNCR1* are highlighted in red, bolded font. The *SLNCR1*$^{\text{AR MUT 1 and 2}}$ expressing plasmid was generated through PCR amplification of *SLNCR1*$^{\text{AR MUT 2}}$ using the indicated plasmids. Duplexed primers containing ATG, FLAG tag and 3x glycine linker are flanked by NheI and AgeI sites to enable cloning into pEGFP-C1-AR. MaP = primers for mutation profiling experiments with SHAPE and DMS reagents.

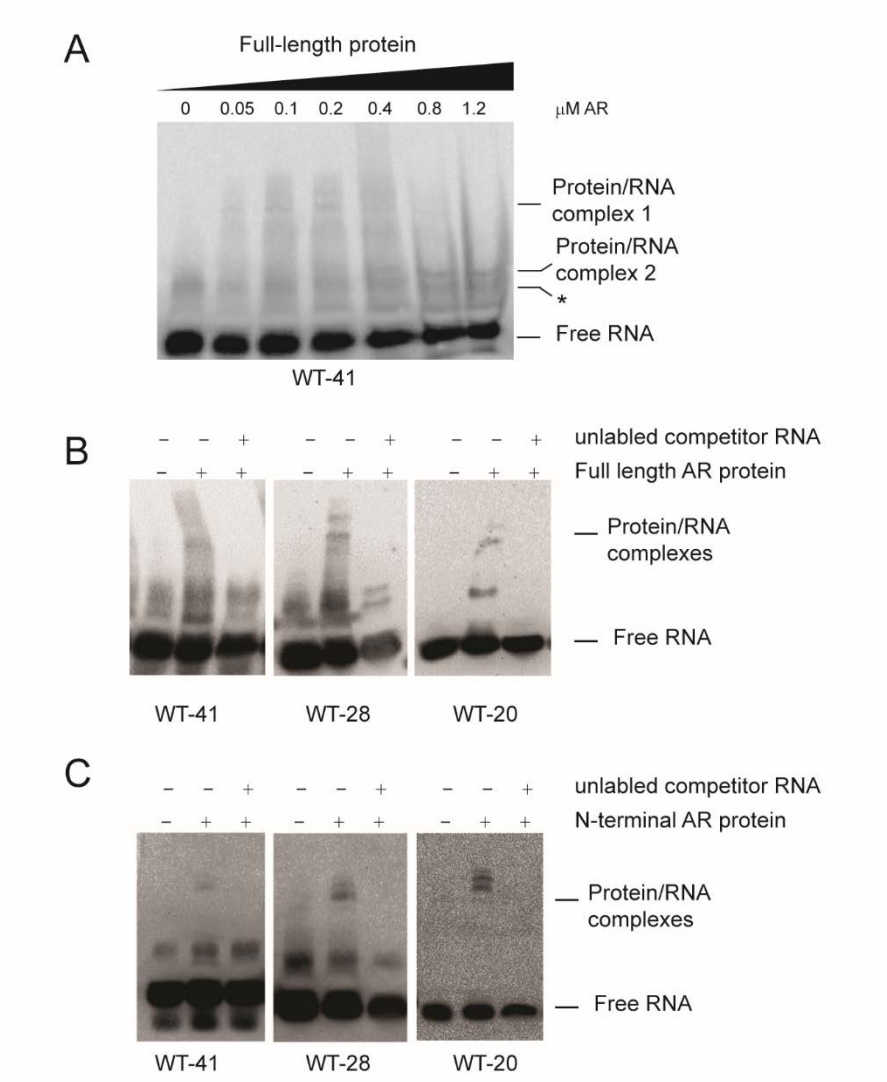

Figure S1: Competition assays confirm that the AR N-terminus specifically binds to biotinylated probes corresponding to WT-41, WT-28, and WT-20. Related to Figure 1. (A) WT-41 probe were incubated with increasing concentrations of full-length AR, resolved on a 5% TBE gel and probed using Streptavidin-HRP following transfer to a negatively charged membrane. The lines indicate either unbound labeled probe or the more slowly migrating RNA-protein complexes. The asterisk denotes a non-specific RNA band. (B and C) Probes were incubated with 600 nM of recombinant (B) full-length AR protein, or (C) AR NTD. Where indicated, 10 μM of unlabeled RNA competitor corresponding to WT-41 was added prior to addition of biotinylated probes. REMSAs were completed as in Figure 1.

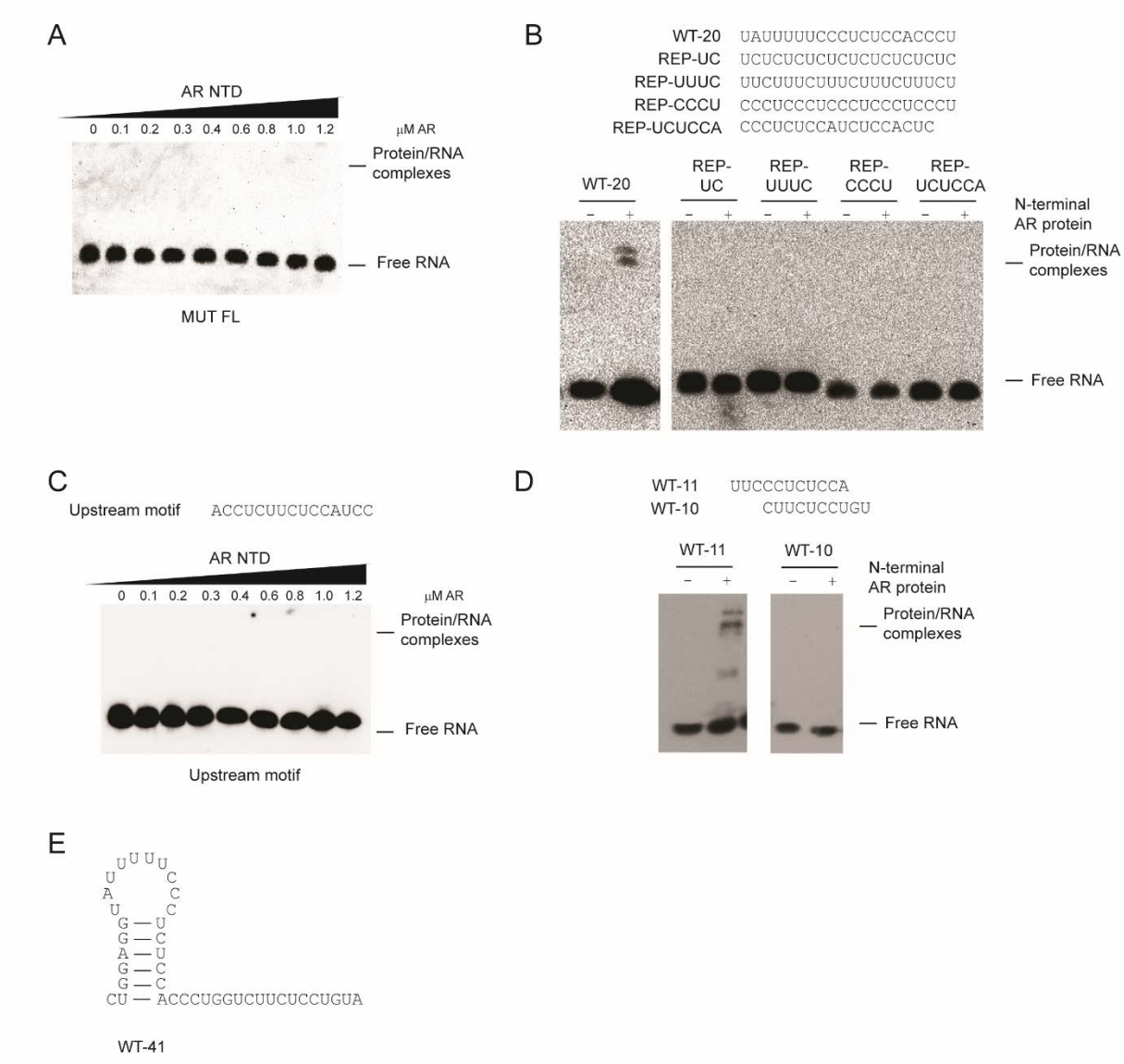

Figure S2: AR does not bind promiscuously to pyrimidine-rich RNAs and requires at least 11 nucleotides to bind. Related to Figure 2. (A and C) The indicated probes were incubated with increasing concentrations (as indicated) of AR NTD, as in Figure 1C. (B and D) REMSAs of the indicated probes incubated with 600 nM of recombinant AR NTD. (E) Secondary structure model of WT-41 (ΔG = -6.1), as predicted by RNAStructure server.

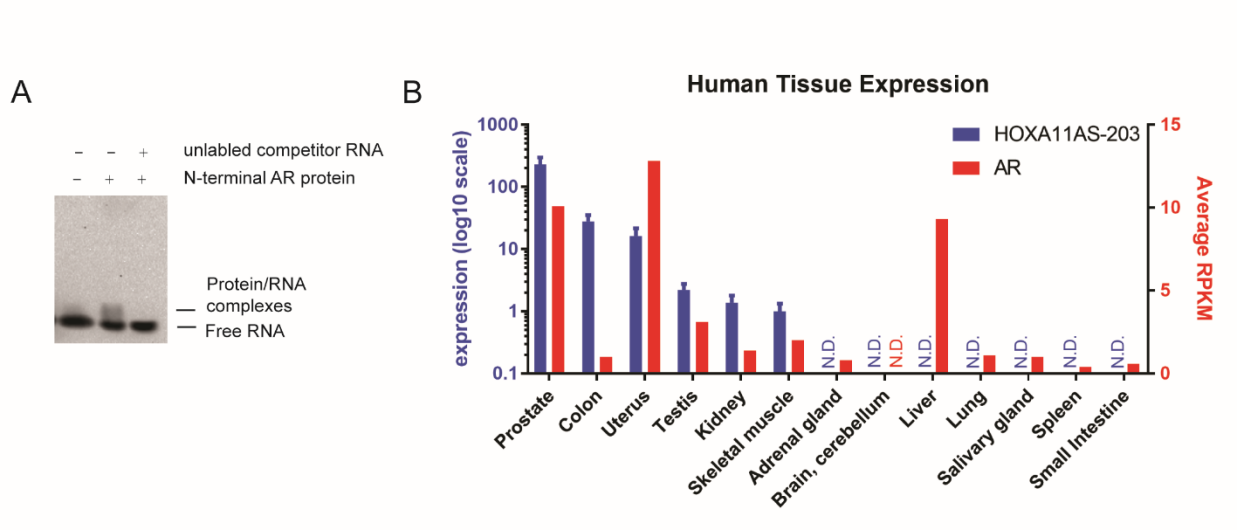

Figure S3: AR NTD region likely directly binds to *SRA1* and *HOXA11AS-203*. Related to Figure 3. (A) A biotinylated probe corresponding to a region of *SRA1* (Figure 6A) was incubated with 600 nM of recombinant AR NTD. In lane 3, 10 µM of unlabeled RNA competitor corresponding to WT-41 was added prior to addition of biotinylated probes. REMSA was completed as in Figure 1. (B) *HOXA11AS-203* is expressed in AR-expressing tissues. Expression of *HOXA11AS-203* was quantified using RT-qPCR with isoform specific primers, represented as the fold change compared to skeletal muscle expression, normalized to GAPDH. Error bars represent standard deviations calculated from 3 reactions. AR mRNA expression is represented as the average RPKM from GTEx RNA-seq, as presented in The Human Protein Atlas.

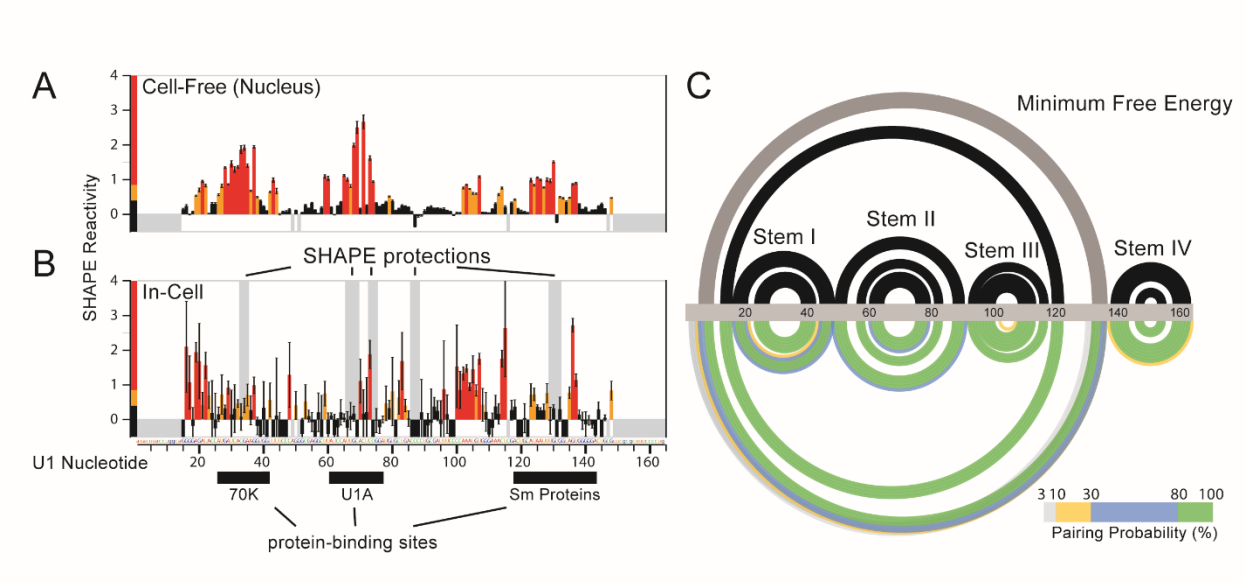

Figure S4: SHAPE-MaP accurately models structure and protein-interaction sites of U1 snRNA. Related to Figure 4. SHAPE reactivity profiles for U1 small nuclear RNA from (A) cell-free extracted nuclear RNA (WM1976 cells) or (B) in-cell experiments. Relative SHAPE reactivities are shown as colored bars (see scale), and standard errors are indicated. Sites of significant in-cell SHAPE protections are indicated as vertical gray bars. 70K, U1A, and Sm protein interaction sites on U1, as visualized in high-resolution structures, are highlighted below (see main text for additional information and references). Grey bars below zero indicate nucleotides included in amplification primers or residues with high background (and are thus classified as no-data). (C) A SHAPE-directed model of the U1 RNA secondary structure is shown. Base-pairing between nucleotides in U1 are represented as colored arcs linking participating nucleotides, including the minimum free energy secondary structure (top) and associated base-pairing probabilities (bottom) indicated by color (see scale). All accepted duplexes are observed in the model (black), and only one extra duplex is predicted (grey) where normally U1 RNA is engaged by proteins in vivo.

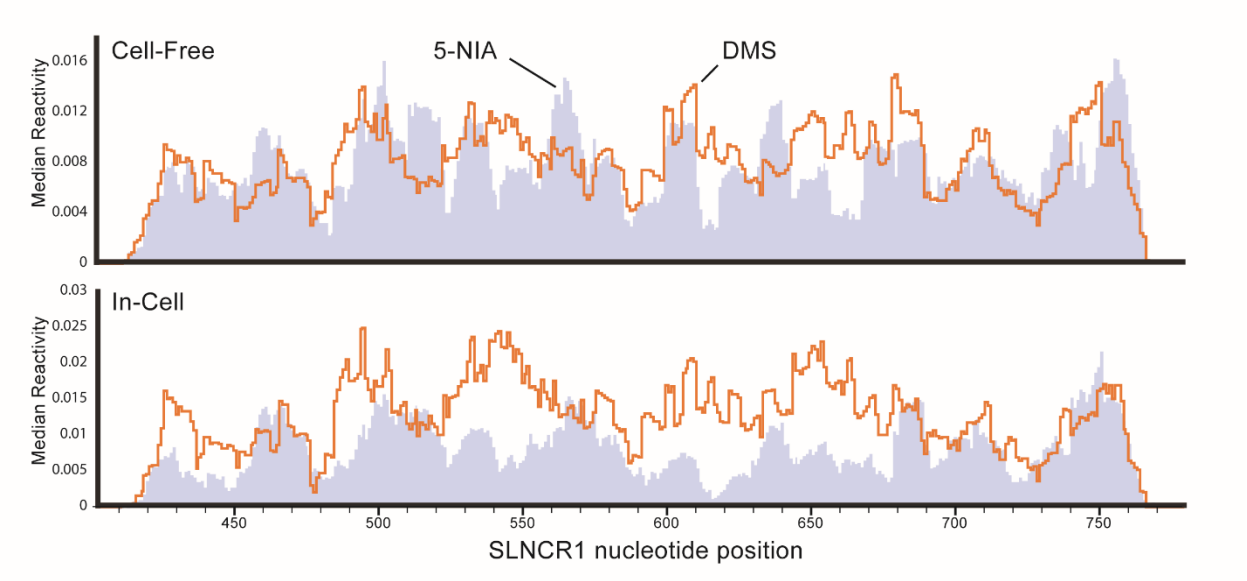

Figure S5: Comparison of SHAPE-MaP and DMS-MaP mutation rates. **Related to Figure 4.** Reactivity profiles for nts 403-720 of *SLNCR1* for cell-free (nucleus) and in-cell SHAPE and DMS-MaP experiments, using RNA from WM1976 cells. Reactivities are displayed a 11 nucleotide windowed medians and 5NIA rates were scaled up by the DMS/5NIA median ratio for ease of comparison. Related to Figure 4. Reactivities compared here are the raw differences of treated and untreated sample mutation rates, as no denaturing control is performed for DMS-MaP experiments.

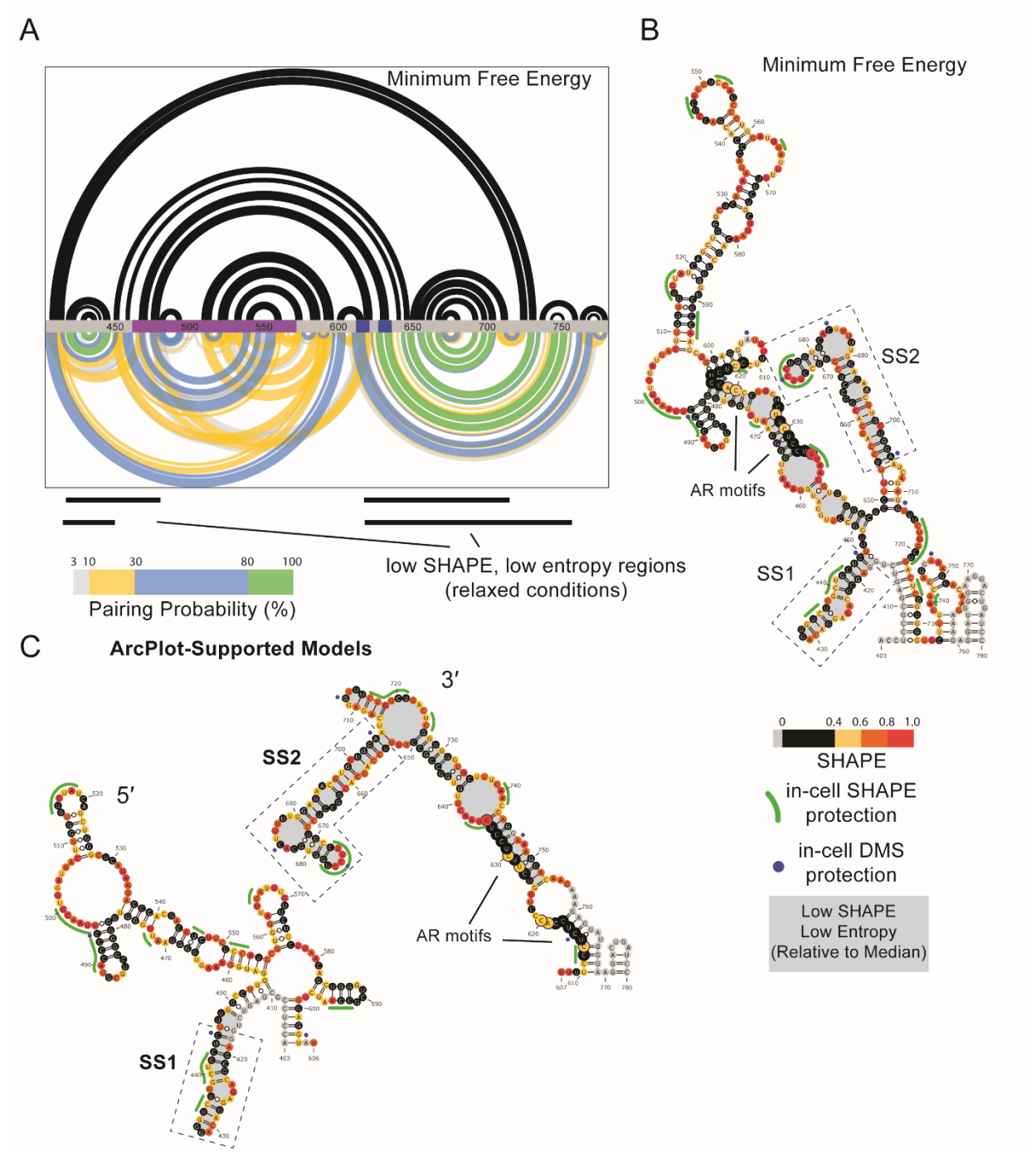

Figure S6: Minimum free energy and alternative secondary structure models of *SLNCR1*$^{403\text{-}780}$. Related to Figure 5. (A) SHAPE-directed secondary structure modeling of nts 403-720 of *SLNCR1*. Base-pairs are represented by colored arcs linking participating nucleotides, including the minimum free energy secondary structure (top) and base-pairing probabilities (bottom). Low SHAPE, low entropy regions, which are relative to the global *SLNCR1* 403-780 median and do not conform to the more stringent thresholds described in the text, are labeled below. Secondary structure projections of the (B) minimum free energy model and (C) arcplot-supported alternative structures are represented with associated SHAPE reactivities and in-cell reagent protections. SS1 and SS2 denote low SHAPE, low Shannon regions 1 and 2 that are maintained in both models, and other low SHAPE, low entropy structures are shaded gray.

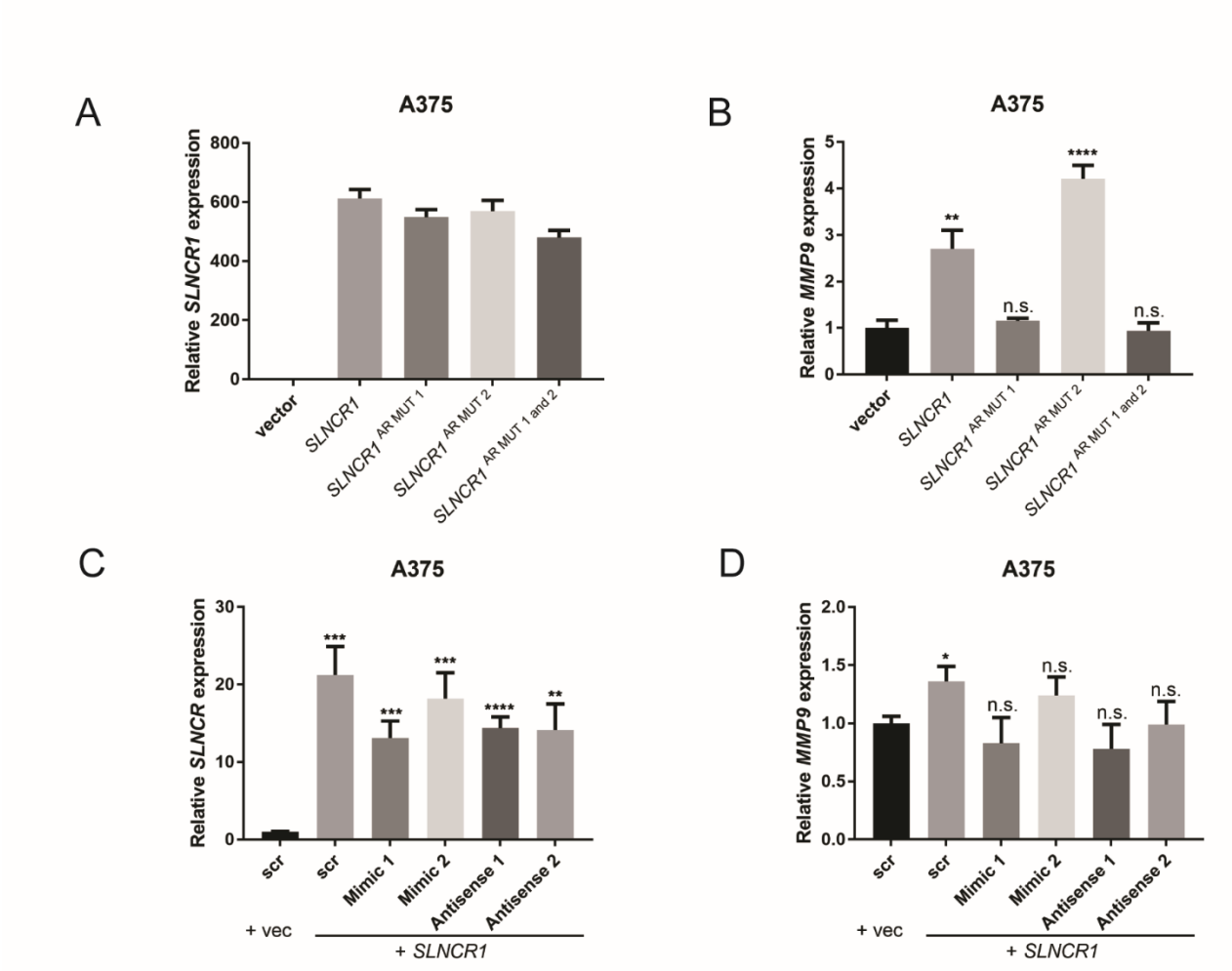

Figure S7: Mutation of AR-binding motifs 1 and 2 or sterically-blocking the AR-*SLNCR1* interaction negates *SLNCR1*-mediated *MMP9* upregulation. Related to Figures 6 and 7. Relative (A) *SLNCR1* transient overexpression or (B) *MMP9* expression in A375 cells transfected with plasmids expressing either wild-type or mutant *SLNCR1*. Relative (C) *SLNCR1* transient overexpression or (D) *MMP9* expression in A375 cells independently transfected with either an empty or *SLNCR1*-expressing plasmid, and following addition of the indicated FANA-modified oligos. RNA was extracted from cells used in invasion assays shown in Figure 7C. A similar degree of *SLNCR1* overexpression was observed for the different conditions, as demonstrated by nonsignificant differences in *SLNCR1* expression between cells treated with scr, Mimic 2, Antisense 1 or Antisense 2 oligos. RT-qPCR data is represented as the fold change compared to A375 vector (A and B) or vector and scramble (C and D) control, normalized to GAPDH. Error bars represent standard deviations calculated from 3 reactions. Significance was calculated using the Student's t-test compared to vector only control (B) or vector/scramble only control (C and D): * p-value < 0.05, ** p-value < 0.005, **** p-value < 0.001, n.s. = not significant.